Spatial and temporal scaling of oxide cluster aggregation on a liquid-gallium surface

Y. L. Wang and S. J. Lin
Institute of Atomic and Molecular Sciences, Academia Sinica, P.O. Box 23-166 Taipei, Taiwan 107, Republic of China
and Department of Physics, National Taiwan University, Taipei, Taiwan 107, Republic of China
(Received 6 November 1995)

Oxide clusters grow spontaneously on a liquid-gallium surface exposed to oxygen at room temperature. Clusters diffuse and aggregate to form larger and larger clusters with a fractal dimension d_f of $\sim$1.5. The total number of clusters and the weighted average cluster size do not exhibit power-law dependence on time, while the typical linear dimension of the clusters exhibits a $t^{1/2}$ time dependence. The exponent appears to be consistent with Binder's prediction for the phase separation of two-dimensional binary fluid mixture. For early stages of the aggregation, the structure function $F(k,t)$ of the oxide patterns can be scaled as $[k_m(t)]^{-d_f} f(k/k_m)$, where k_m is the peak position of $F(k,t)$ and $f(k/k_m)$ is a time-independent function. However, such a scaling behavior, which is a generalization of Furukawa's theory for spinodal decomposition, does not hold for longer times.

I. INTRODUCTION

When a liquid-metal surface is exposed to oxygen, oxidation takes place spontaneously and oxide particles are formed on the surface. Because the diffusivity of oxide particles on a liquid surface is usually much higher than on a solid surface, an oxide growth process on a liquid surface is expected to be very different from that on a solid surface. Interesting phenomena including long-range diffusion and aggregation of oxide particles could take place. The process of oxide pattern formation in such a diffusion-reaction system constitute a complex and fascinating subject by itself. It is therefore quite remarkable to note that liquid-metal oxidation is a subject that has been rarely studied. Only recently have some related experiments been reported.[1–3]

An important step toward understanding an oxide pattern formation process on the surface of a liquid metal is to study its spatial and temporal scaling properties. The information can provide us with not only some basic rules for describing the lateral oxide growth kinetics but also insights into the growth mechanism. Furthermore, if similar scaling properties could be found in other types of systems, our understanding of the process would be greatly improved by simply addressing the similarities and differences between the two types of systems. In this paper, we report our study of the lateral oxide pattern formation on a liquid-gallium surface with an emphasis on its spatial and temporal scaling properties. We found that the oxide clusters aggregate among themselves to form self-similar patterns. And the typical linear dimension of the clusters and structure function of the oxide patterns also exhibit interesting temporal scaling properties. Specifically, we try to understand these scaling properties using a theoretical framework that has been developed for describing spinodal decomposition of a binary alloy. Some of the results are also compared with computer simulations based on different models of cluster aggregation.

II. EXPERIMENTAL

Gallium has been chosen for this study because it has a very low vapor pressure ($<10^{-11}$ Torr) at its melting point. This is essential to the experiment because oxidation of a liquid-gallium surface occurs spontaneously when exposed to oxygen at a room temperature of $\sim$20 ° C. A liquid-Ga sample was prepared by heating a piece of high purity (99.999%) Ga ingot on a stainless substrate to a temperature slightly above its melting point. The area and the thickness of the sample was about 1 cm^2 and 0.5 mm, respectively. Without appropriate seeding, Ga remains liquid at room temperature for an indefinite time. Right before the sample was loaded into the scanning focused ion-beam (FIB) system used for this study, the native oxide layer, primarily Ga_2O_3,[4] was scraped away, creating an optically brilliant surface. Great care was taken to ensure the liquid surface remained smooth and balanced during the sample transfer and throughout the experiment. After the sample was loaded into the analysis chamber, the FIB was operated at a high current (5 nA) mode in order to sputter clean a $(3\ mm)^2$ area on the surface. The typical time needed for the sputtering is $\sim$20 h. Since the FIB column employs Ga ions, the purity of the Ga sample surface after the *in situ* sputter cleaning was preserved. The base pressure of the FIB chamber was 1×10^{-10} Torr, which essentially halted the oxidation process because no oxide growth was observed on a cleaned Ga surface after it was left in a pressure of 2×10^{-9} Torr for several days.

Ions extracted from a liquid-Ga source are accelerated to 25 keV and focused by the two electrostatic lens to form a beam with an electronically variable diameter between 30 nm to several microns. Two octopole scanners are employed to raster the beam across the sample and correct the astigmatism of the optical column. Secondary ions ejected by the FIB are detected by a channel electron multiplier overlooking the target area. The beam scanning, data acquisition, and image processing are achieved using a personal computer with in-house developed software.[3,5] For secondary ion imaging analysis, the FIB is scanned across the sample with a fixed dwell time on each pixel element, and the number of ion pulses recorded by the detector during this period of time is translated into the gray level of the corresponding pixel of a picture. Typically, images are stored digitally in array of 512×512 pixels.

The oxidation of the cleaned liquid Ga was achieved by backfilling the chamber with O_2 (99.9999%) to a pressure of 1×10^{-7} Torr. During the typical oxygen exposure period of a few minutes, the FIB was blanked to avoid disturbing the growth. After the exposure, the oxygen was evacuated from the chamber and the pressure decreases below 1×10^{-9} Torr in less than a few minutes.

Because of the destructive nature of the ion-beam imaging analysis, the FIB was deliberately defocused and operated in a very low current mode to minimize the disturbance to the oxide growth process. With a beam current of 16 pA and a beam diameter of ~1 μm, the instant beam current density is 2 mA/cm^2. Under such a beam for a typical well time of 100 μs, the total dose received by each pixel element on the sample is $\sim1\times10^{12}$ (ions/cm^2). Essentially, this low dose ion-beam analysis is known as static secondary ion mass spectrometry (SIMS).[6] The beam diameter was deliberately set at ~1 μm to serve another purpose. For a 512×512 pixels scan over an area of (560 μm)^2, this beam diameter is about the same as the spacing between neighboring pixels on the sample. Such an arrangement ensures that the areas scanned by the ion beam are almost consecutive, and the acquired image is a better representation of the object.[7,8] Also to be noted is that the average beam current density on the scanned area is only ~5 nA/cm^2, and therefore the thermal effect due to the ion-beam bombardment is negligible. To further reduce the disturbance caused by the ion bombardment, all the images of the oxide pattern were taken from different area in the (3 mm)^2 sample surface. (Only prolonged imaging of the same area resulted in observable disturbance to the oxide growth process.)

In principle, it is more straightforward to use secondary oxygen ion signals for imaging the location of gallium oxide particles on the surface. However, because most of the sputtered oxygen leaves the surface in either neutral or negative charge states, the oxygen-ion signal was found to be much weaker than positive Ga-ion signal. Therefore, we chose to use the Ga^+ signal to locate the position of the gallium oxide particles. This seemingly counterintuitive approach is possible because the ionization probability of a metallic atom sputtered from its oxide phase is usually much higher than from its pure phase. This effect of so called ''oxygen enhancement'' is well documented in the field of SIMS.[6] It has been clearly demonstrated in previous studies[1–3] of gallium oxidation. In this experiment, we found that the average secondary ion signal emitted from gallium oxide particles is ~5 times greater than that from the cleaned gallium surface. This difference in signal intensity allows us to select a threshold level for a high-pass filter. It is then used to transform a secondary ion image into a binary map with the 1's representing the sites occupied by oxide and 0's by the clean gallium surface.

III. RESULTS AND DISCUSSION

Figure 1 shows a typical oxide aggregation process at different times after the exposure of 25 L of oxygen. We have chosen this exposure because it leads to an oxide fractional coverage of $\sim10\%$ and a growth process at this coverage takes place in a manageable time scale. From these images, it is clear that, a few minutes after the oxygen exposure, small oxide clusters on the order of a few micron in size are formed on the gallium surface. Gradually, these clusters diffuse and aggregate among themselves to form larger and larger clusters. At the latter stages, oxide clusters spanning over an area as large as (~100 μm)^2 are formed on the surface. To be noted in particular is that, although the size and span of the clusters increases with time, the typical width of an individual oxide ''fiber'' remains approximately the same ($1\sim2$ μm) and the fractional surface oxide coverage also remains almost constant. This observation suggests that, once the micron-size clusters are formed in the initial stage, all the oxygen adsorbed by the surface is stored in the oxide clusters. The time evolution of the oxide pattern is determined primarily by the diffusion and aggregation of the oxide clusters.

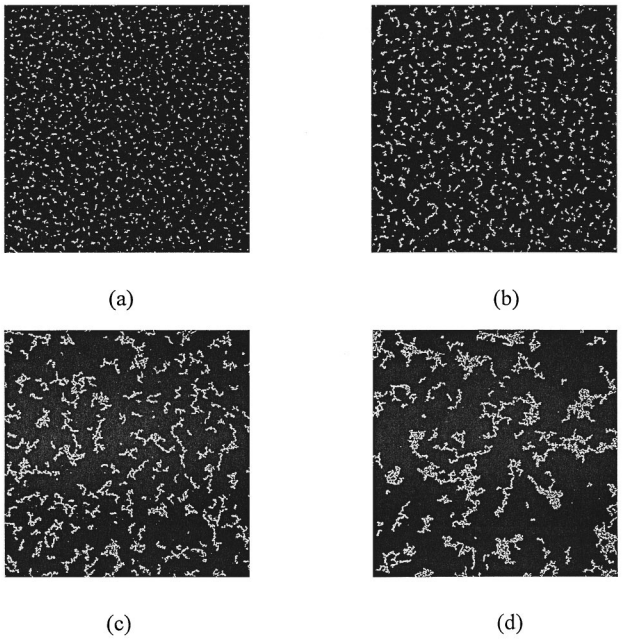

FIG. 1. Binary images of oxide clusters (bright) on a liquid-Ga surface at different stages of the aggregation process. The oxygen exposure is 25 L and the times are (a) $t=5$ min, (b) $t=14$ min, (c) 64 min, (d) 94 min. Full scale of the images is 560 μm and each picture consists of 512×512 pixels.

The basic kinetics of a cluster aggregation process can be described by the time dependence of two quantities: the total number of the clusters $N(t)$ and the weighted average cluster size S. The latter is defined as

$$S(t)=\frac{\sum s^2 n_s(t)}{\sum s n_s(t)}, \tag{1}$$

where n_s is number of clusters with size s. In this experiment, s is defined to be the number of pixels covered by a cluster. As shown in Figs. 2(a) and 2(b) the total number of clusters decays with time. However, it does not follow a simple power-law decay. We have attempted to fit the data to well-known functions such as exponential decay without much success. The best fit seems to be a logarithmic decay as shown in Fig. 2(b). According to previous Monte Carlo

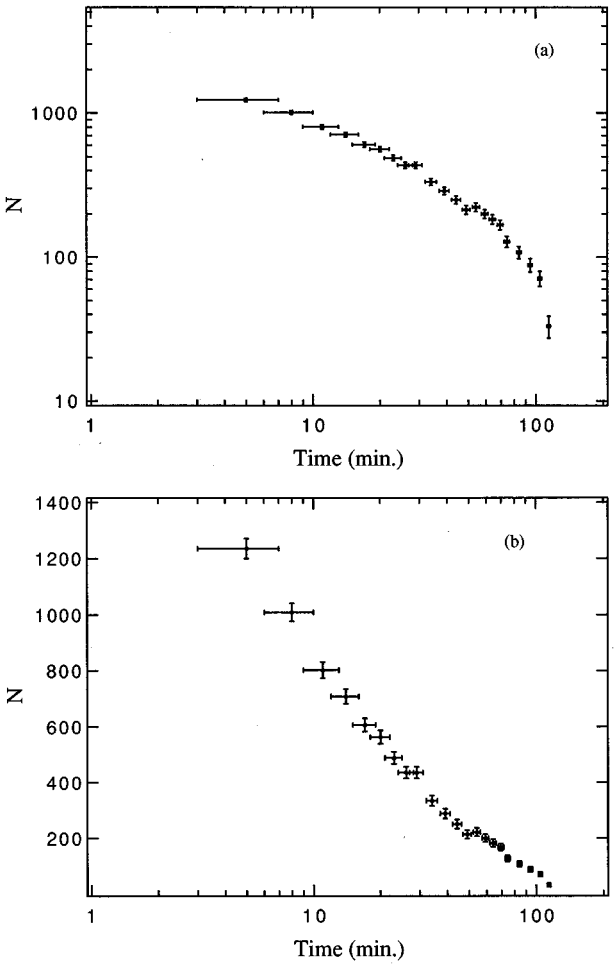

FIG. 2. Total number of clusters in an area of (560 μm)^2 as a function time. Data are plotted in (a) log-log and (b) linear-log scale.

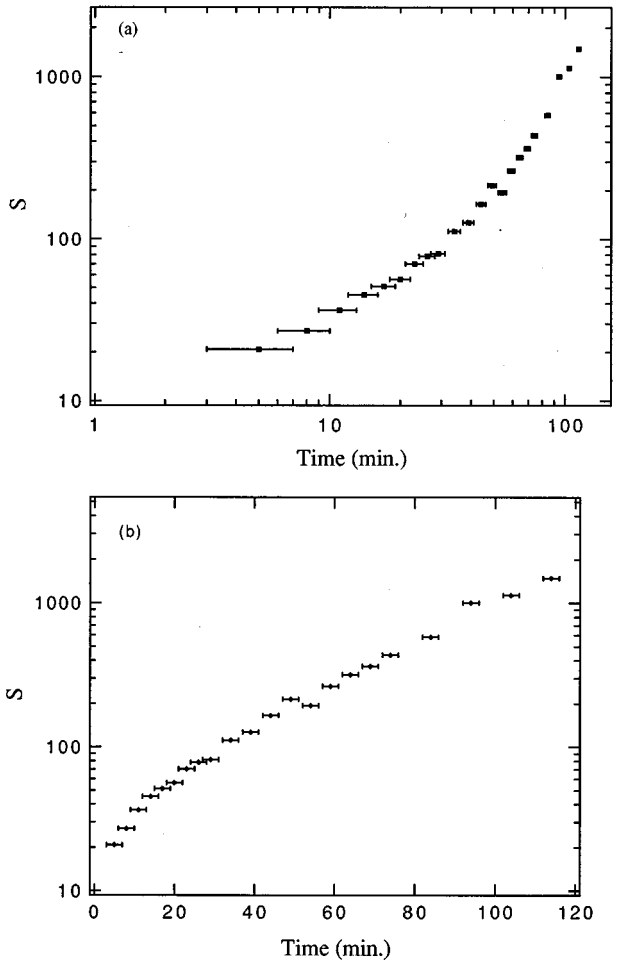

FIG. 3. Weighted average cluster size of the clusters in an area of (560 μm)^2 as a function time. Data are plotted in (a) log-log and (b) log-linear scale.

simulations,[9–12] a power-law dependence of $N(t)$ is expected if the process is a diffusion-limited cluster-cluster aggregation (DLCCA). Figures 3(a) and 3(b) show the time dependence of S. Again, S does not increase with time according to power law as suggested by the computer simulations of DLCCA. The observation that S increases exponentially with time appears to be closer to the results of a simulation based on reaction-limited cluster-cluster aggregation (RLCCA). In this model, the probability that two clusters will combine depends only on the time that they spend in contact with each other.[11] Similar exponential growth of S has been observed in a variety of experiments under slow aggregation conditions.[13–15]

To derive the spatial scaling property of the oxide patterns, we have plotted the size (s) of the clusters versus their radii of gyration (R_g) in Fig. 4. It shows that $s \propto R_g^{-d_f}$ can be established and therefore the oxide aggregation process leads to the formation of self-similar clusters with a fractal dimension d_f of 1.53 ± 0.06. According to available computer simulations, $d_f = 1.44 \pm 0.04$ and 1.55 ± 0.03 for DLCCA and RLCCA, respectively.[16] Although the result appears to be closer to RLCCA, we would like to be more cautious about such a conclusion. In the computer simulations, clusters are assumed to be rigid and the effects of the deformation and relaxation of clusters are not included. Such internal rearrangement of a cluster could effectively change its morphology from a more ramified DLCCA-like structure to a more compact RLCCA-like structure.

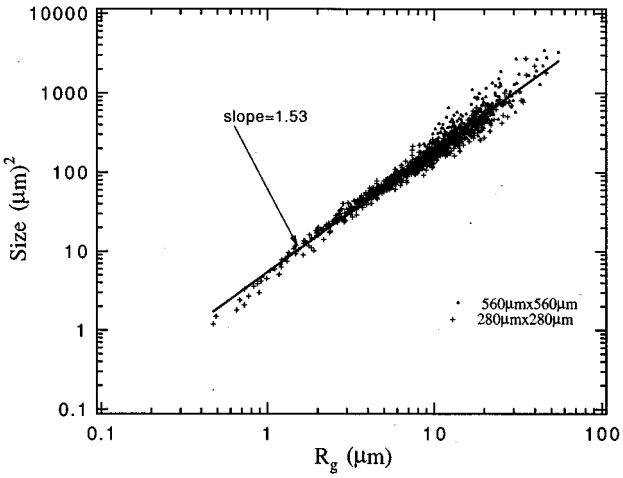

FIG. 4. Area occupied by a cluster versus its radius of gyration. Data are taken from images (512×512) at two different magnifications.

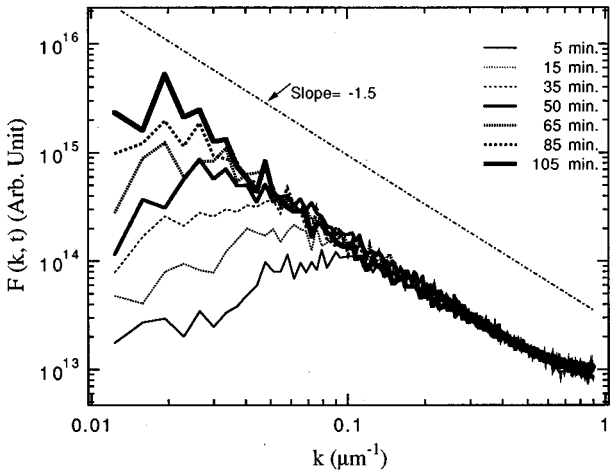

FIG. 5. Structure function of the oxide patterns in an area of (560 μm)^2. The straight line represents a function proportional to $k^{-1.5}$. It is included to help demonstrate the power-law behavior of F at large wave numbers.

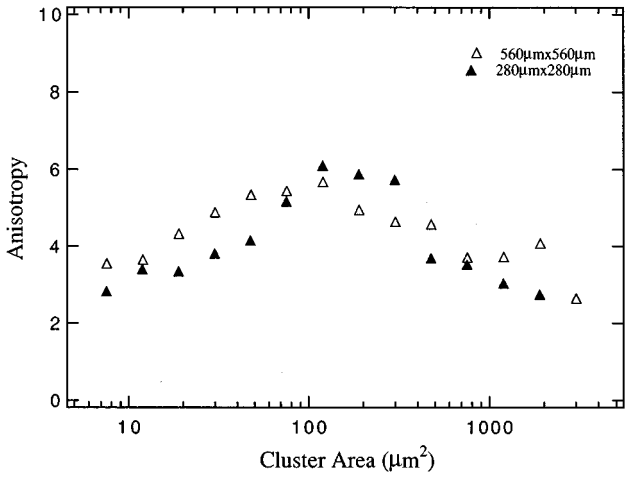

FIG. 6. Cluster anisotropy versus its area. Data are taken from images (512×512) at two different magnifications.

The fractal dimension of a pattern can also be derived from its density-density correlation function,

$$C(r)=\frac{1}{M}\sum_{\mathbf{r}'}\rho(\mathbf{r}+\mathbf{r}')\rho(\mathbf{r}'), \tag{2}$$

where $\rho(\mathbf{r})$ is the local density, representing the probability (0 or 1) that the site is occupied by particles. For a self-similar pattern, the angular average of $C(\mathbf{r})$ decays as

$$C(r)\propto r^{d_f-d}, \tag{3}$$

where d is the dimensionality. Since $C(r)$ of a pattern is equivalent to the inverse Fourier transformation of its power spectrum $F(k)$, it is straightforward to show that the structure function of a self-similar pattern decays as

$$F(k)\propto k^{-d_f}, \tag{4}$$

We have shown $F(k)$ of the oxide pattern at different times in Fig. 5. The power-law decay behavior at large wave number again indicates that the oxide patterns are made of an ensemble of clusters with a fractal dimension of $\sim$1.5, in agreement with the above results derived from the radii of gyration. Also to be noted is that each $F(k,t)$ exhibits a peak at $k=k_m$. This indicates that the self-similarity of the clusters is limited to a length scale below $\sim k_m^{-1}$. As the sizes of the clusters increase, k_m shifts towards smaller wave numbers, while its tail at large wave number remains approximately proportional to k^{-d_f}.

Besides its fractal dimension, the anisotropy of a cluster can also provide information about its morphology. Mathematically, the anisotropy of a cluster can be defined as

$$A=\frac{\langle R_L^2\rangle}{\langle R_S^2\rangle}, \tag{5}$$

where R_L and R_S are the largest and the smallest principal radii of gyration of a cluster, respectively, and the brackets represent ensemble average. According to Botet and Jullien's numerical simulation,[17] $A=5.7\pm0.2$ and 4.7 ± 0.2 for DLCCA and RLCCA, respectively. Figure 6 shows the average anisotropy of clusters as a function of their sizes. If we neglect the apparent size dependence of the anisotropy and take the grand average of $A=4.2\pm0.7$ as the average anisotropy of the oxide clusters, the results would again indicate that the aggregation process is closer to RLCCA. However, neither DLCCA nor RLCCA simulation results in significant size dependence of A. We therefore think that neither model is adequate for describing the oxide aggregation kinetics. Although we do not know exactly what causes the size dependence of A, we believe that the decrease of A as clusters grow larger than $\sim$100 μm^2 is related to the increase of their flexibility with increasing size. A flexible cluster could reduce both its anisotropy and fractal dimension through relaxation and deformation. Unfortunately, to our knowledge, the effects caused by such internal rearrangement of a cluster have not been taken into account in the simulations available to date.

The time dependence of the typical cluster linear dimension (k_m^{-1} or R_g) is another important quantity essential to describing the aggregation kinetics. The results of our experiment (Fig. 7) indicate that average $\langle R_g\rangle$ is approximately proportional to $t^{1/2}$. Apparently, this power law is so simple that a semiquantitative explanation is in order. In the following, we will try to elucidate a possible origin of this power law. Our analysis is based on a theoretical framework that has been developed for spinodal decomposition of a binary alloy. For details of this subject, readers are referred to Furukawa's comprehensive review.[18] Heuristically, these theories, which originated from Binder and Stauffer,[19] assume a Smoluchowski-type kinetics for the cluster coarsening process. Each cluster is regarded as a Brownian particle, and travels freely until it meets another. Once two clusters meet, they coalesce into one larger cluster. Let D_R be the diffusion coefficient of a cluster with a typical radius R. If one assumes that the average distance between neighboring clusters is proportional to the average cluster radius R, then

$$D_R\propto\frac{R^2}{\Delta t}, \tag{6}$$

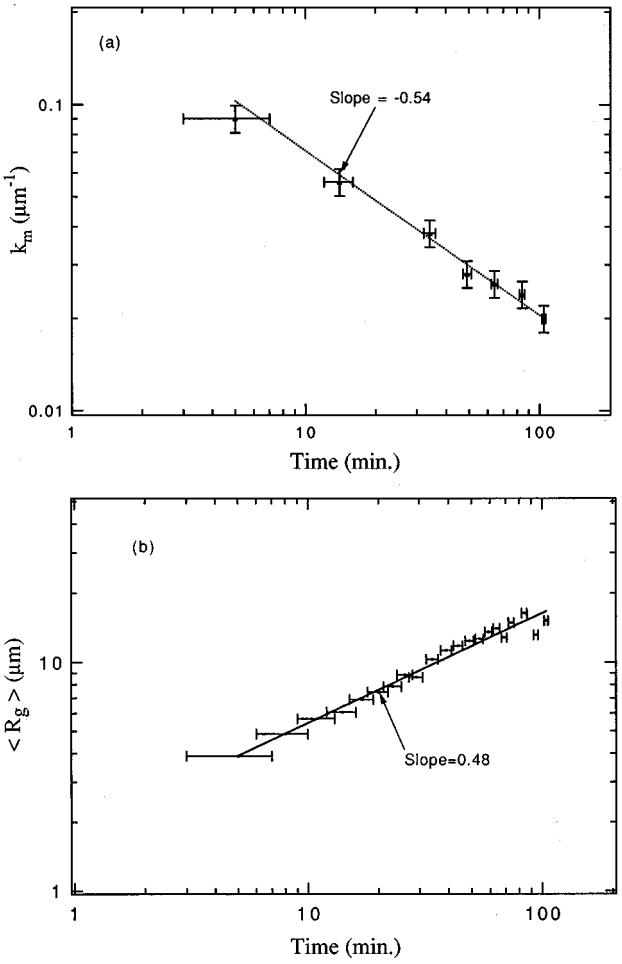

FIG. 7. The time dependence of the characteristic cluster linear dimension: (a) peak of the structure function, (b) average radius of gyration. Straight lines are power-law fits to the data.

where Δt is the mean free time for a cluster to travel. Since the cluster radius increases by an amount of the order R after each coalescence, the rate of increment of the radius can be approximated by

$$\frac{\Delta R}{\Delta t} \propto \frac{R}{\Delta t} \propto \frac{D_R}{R}. \tag{7}$$

(To be noted is that $\Delta R \propto R$ remains valid for the aggregation of fractal-like clusters with a definitive fractal dimension.) If one assumes that

$$D_R \propto R^{-x}, \tag{8}$$

it is straightforward to derive from Eqs. (7) and (8) that $R(t)$ ($\propto k_m^{-1}$) has a power-law behavior as

$$R(t) \propto t^{1/(x+2)}. \tag{9}$$

Many theories have been proposed to estimate the exponent x for both solid and liquid mixture at various conditions.[20,21] For example, in one of Binder's theories, the diffusion of a cluster in a solid mixture is assumed to be caused by the exchange of two kinds of atoms on its surface, and therefore $x=d+1$ is estimated, which results in a $R \propto t^{1/(d+3)}$ dependence. In one of Furukawa's models, $x=d$ is suggested, which leads to $R \propto t^{1/(d+2)}$. For a d-dimensional liquid mixture, Binder suggested a general $R \propto t^{1/d}$ dependence.[20] For $d=3$, this prediction can be understood using the following heuristic arguments. According to Stoke's law, the mobility of a sphere in a liquid is proportional to R^{-1}. Based on Einstein's relation between the diffusion coefficient and the mobility,[22] one can easily show that $D_R \propto R^{-1}$. Therefore, $R \propto t^{1/3}$ is predicted for the aggregation of three-dimensional (3D) clusters in a 3D liquid. To our knowledge the mobility of a 2D object moving in a 2D liquid has not been explicitly calculated,[23] it is not clear how Binder has derived the general $R \propto t^{1/d}$ dependence.[20] Nevertheless, the prediction appears to be consistent with our results for $d=2$. This could be an experimental result that appears to be consistent with Binder's prediction for the clustering of a binary fluid mixture in two dimensions.

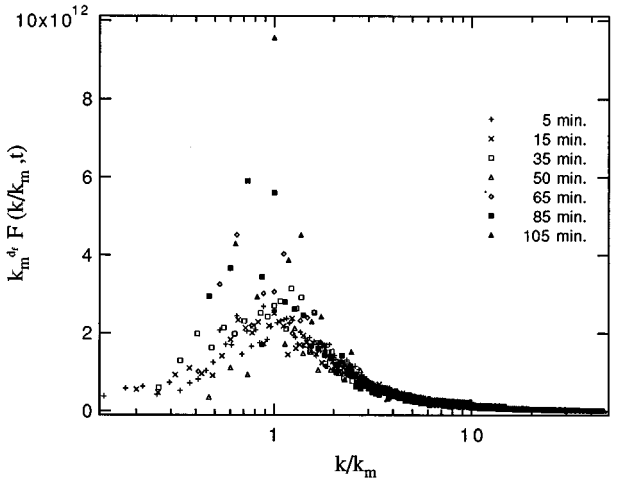

FIG. 8. Rescaling of the structure function according to Eq. (11).

In the study of spinodal decomposition, another important issue of concern is the time evolution of the structure factor $F(k,t)$ of a system. Furukawa[21] has suggested that F scales according to the following law:

$$F(k/k_m, t) = k_m^{-d}(t) f(k/k_m), \tag{10}$$

where $k_m(t)$ is the peak position of $F(k,t)$ at different time, and $f(k/k_m)$ is a time-independent scaling function. It is therefore interesting to try to examine if similar scaling exists in other types of cluster formation processes.[24–26] Because $F \propto k^{-d_f}$ for $k \gg k_m$ in our system, the only possible analogy to Eq. (10) that will keep the tails of $F(k/k_m, t)$ invariant after rescaling of the k axis is of the following form:

$$F(k/k_m, t) = k_m^{-d_f}(t) f(k/k_m). \tag{11}$$

Plotted in Fig. 8 is the rescaling of F according to Eq. (11). It clearly shows that the generalized scaling law of Furukawa is only approximately applicable to our system within a limited initial period of aggregation. Based on these results and the failure of previous attempts to rescale the structure functions of other systems using Eq. (11),[26] it seems likely that the idea that only one unique length scale is enough to describe the evolution of a system over the entire aggregation process is not adequate.

In conclusion, we have studied the spatial and temporal scaling of the aggregation of gallium oxide particles on a liquid-gallium surface. We found that oxide clusters diffuse on the surface and aggregate to form larger and larger fractal-like clusters. By comparing the experimental results: the time dependence of the total cluster number and the weighted average cluster size; the fractal dimension and anisotropy of the clusters, with computer simulations, the oxide aggregation process appears to be closer to a reaction-limited cluster-cluster aggregation process. However, because the effects caused by cluster internal rearrangement are not included in the simulations, this conclusion should be taken with caution. The time dependence of the typical cluster linear dimension exhibits a simple $t^{1/2}$ power-law behavior, which appears to be consistent with Binder's prediction for the phase separation of two-dimensional binary fluid mixture. Further experimental and theoretical efforts are needed to clarify the validity and implications of this interesting observation. In the early stages of aggregation, the structure function of the oxide patterns exhibits a universal scaling behavior analogous to that of spinodal decomposition. However, this temporal scaling, which represents a generalization of Furukawa's theory for spinodal decomposition, does not hold for longer times. The result suggests that more than one unique length scale might be needed for describing the evolution of a system over the entire aggregation process.

ACKNOWLEDGMENTS

This work is supported by the National Science Council (Contract No. 83-0208-M-001-108), Taiwan, Republic of China.

[1] Y. L. Wang, A. Raval, and R. Levi-Setti, Scanning Microsc. **3**, 731 (1989).
[2] J. M. Chabala, Phys. Rev. B **46**, 11 346 (1992).
[3] Y. L. Wang, Y. Y. Doong, T. S. Chen, and J. S. Haung, J. Vac. Sci. Technol. A **12**, 2081 (1994).
[4] C. Y. Su, P. R. Skeath, I. Lindau, and W. E. Spicer, Surf. Sci. **118**, 248 (1982).
[5] Y. L. Wang and Z. Shao, in *Advances in Electronics and Electron Physics*, edited by P. W. Hawkes (Academic, Boston, 1991), Vol. 81, pp. 177–209.
[6] A. Benninghoven, F. G. Rudenauer, and H. W. Werner, *Secondary Ion Mass Spectrometry* (Wiley, New York, 1987).
[7] R. Levi-Setti, Y. L. Wang, and G. Grow, J. Phys. (Paris) Colloq. **45**, C9-179 (1984).
[8] J. M. Chabala, R. Levi-Setti, and Y. L. Wang, Appl. Surf. Sci. **32**, 10 (1988).
[9] P. Meakin, Phys. Rev. Lett. **51**, 1119 (1983).
[10] M. Kolb, R. Botet, and R. Jullien, Phys. Rev. Lett. **51**, 1123 (1983).
[11] T. Vicsek and F. Family, Phys. Rev. Lett. **51**, 1123 (1983).
[12] P. Meakin and F. Family, Phys. Rev. A **38**, 2110 (1988).
[13] M. H. Ernst, in *Fractal in Physics*, edited by L. Pietronero and E. Tosatti (Elsevier Science, Amsterdam, 1986), p. 289.
[14] D. W. Schaefer, J. E. Martin, D. J. Cannell, and P. Wiltzius, Phys. Rev. Lett. **52**, 1416 (1984).
[15] D. A. Weitz, J. S. Huang, M. Y. Lin, and J. Sung, Phys. Rev. Lett. **54**, 1416 (1985).
[16] R. Jullien and R. Botet, in *Aggregation and Fractal Aggregates* (World Scientific, Singapore, 1987), p. 88.
[17] R. Botet and R. Jullien, J. Phys. A **19**, L907 (1986).
[18] H. Furukawa, Adv. Phys. **34**, 703 (1985).
[19] K. Binder and D. Stuffer, Phys. Rev. Lett. **33**, 1006 (1974).
[20] K. Binder, Phys. Rev. B **15**, 4425 (1977).
[21] H. Furukawa, Phys. Rev. Lett. **43**, 136 (1979).
[22] L. D. Landau and E. M. Lifshitz, *Fluid Mechanics*, 3rd ed. (Pergamon, New York, 1977), p. 228.
[23] H. Lamb, *Hydrodynamics* (Cambridge University Press, Cambridge, 1932), p. 184.
[24] D. J. Robinson and J. C. Earnshaw, Phys. Rev. A **38**, 2055 (1992).
[25] D. J. Robinson and J. C. Earnshaw, Phys. Rev. Lett. **71**, 715 (1993).
[26] M. Carpineti and M. Giglio, Phys. Rev. Lett. **68**, 3327 (1992).